



Dissociation of methanol on hydroxylated TiO₂-B (1 0 0) surface: Insights from first principle DFT calculation

Weijia Liu^a, Jian-guo Wang^b, Xiaojing Guo^a, Wei Fang^a, Mingjie Wei^a, Xiaohua Lu^{a,*}, Linghong Lu^a

^a State Key Laboratory of Materials-Oriented Chemical Engineering, Nanjing University of Technology, Nanjing 210009, China

^b College of Chemical Engineering and Materials Science, Zhejiang University of Technology, Hangzhou 310032, China

ARTICLE INFO

Article history:

Received 14 September 2010

Received in revised form 9 January 2011

Accepted 10 January 2011

Available online 3 February 2011

Keywords:

Methanol

TiO₂-B (1 0 0)

Surface hydroxyl group

Dissociation

Formaldehyde

Ab initio

ABSTRACT

The adsorption of methanol on hydroxylated TiO₂-B (1 0 0) surface with bridging and terminal hydroxyl groups has been studied by first principle calculations. On both clean and hydroxylated surfaces with bridging OH group (OH_{br}), the O–H bond scission is the most favorable dissociation of methanol and the C–O bond scission is also feasible. This indicates the OH_{br} has little influence on the adsorption of methanol. The terminal OH group (OH_t) plays a major role in the C–H scission of methanol, which is important for the applications associated with the direct use of hydrogen, such as *in situ* hydrogenation, and hydrogen generation via the photocatalytic reaction. The dissociative adsorption of methanol via C–H scission, which is an endothermic adsorption on other TiO₂ surfaces, is identified as exothermic adsorption with adsorption energy in the range of –1.54 eV to –1.91 eV around OH_t on TiO₂-B (1 0 0) surface. The lowest activation barrier for C–H scission is ~0.80 eV, which is lower than the release heat of molecular adsorption. Moreover, the hydrogen atoms in methanol are easily transferred to the OH_t and then move to nearby O_{2c} sites to regenerate the hydroxyl group. This proton migration process could result in extra stable chemi-sorption of methanol with an adsorption energy as low as –2.23 eV, which is above twice that of methanol molecularly adsorbed on the surface. Thus, the proton channel feature of OH_t on the surface is borne out by our calculations.

© 2011 Elsevier B.V. All rights reserved.

1. Introduction

Due to the energy and environmental crisis, especially global warming, searching for alternative and renewable energies is an urgent mission. Methanol, which is currently recognized as a convenient liquid fuel and feedstock of chemical industry, was recently proposed as next generation energy source beyond oil and gas because of its high volumetric theoretical energy density and high hydrogen capacity (12.5 wt%) [1,2].

Many advanced technologies aiming at making better use of methanol as an energy source are under development [3,4], such as production of hydrogen via photocatalysis or steam reforming method, *in situ* hydrogenation method, and direct methanol fuel cell. Methanol is also an important raw material for the synthesis of olefins, dimethyl ether, etc. [5–7].

TiO₂ supported with noble metals plays an important role in all the above technologies. Like other reactive substrates, such as ZnO [8], ZrO₂ [9], TiO₂ not only could disperse and stabilize the nanoparticles of the noble metal, but also could play an important part in the catalysis reaction [10,11]. Moreover, the TiO₂ substrate with an

exposed reactive surface, for example, anatase (0 0 1), could further improve the catalysis performance [12]. Thus the chemi-sorption and reaction mechanism on the surface of the substrate is critical in understanding the role of reactive substrate in the methanol utilization.

Water and oxygen are always presented in most applications associated with the utilization of methanol. Water is even found to be helpful for the photocatalytic hydrogen generation process from methanol [13]. Mean while on exposure to the moisture or oxygen atmosphere, bridging and terminal hydroxyl groups could form on the TiO₂ surfaces and further impact the chemistry of the surface [14–16]. Thus, the chemi-sorption of methanol on hydroxylated TiO₂ surfaces with different hydroxyl groups is another important aspect to understand the molecular process on the substrates.

Current investigations on the adsorption of methanol on TiO₂ surfaces are mainly focused on anatase, brookite and rutile TiO₂. Only O–H and C–O scissions are predicted to be feasible on the clean or hydroxylated TiO₂ surface [17–19]. Since there are three C–H bonds, which fixate 75% of hydrogen in methanol, the understanding of the C–H scission could be very meaningful in making better use of methanol. C–H activation of organic molecule is also a long-standing problem of major interest [20].

Our preliminary experimental and theoretical study [21–23] showed that TiO₂-B (1 0 0) could be identified as another reac-

* Corresponding author. Tel.: +86 25 83588063; fax: +86 25 83588063.

E-mail address: xhlu@njut.edu.cn (X. Lu).

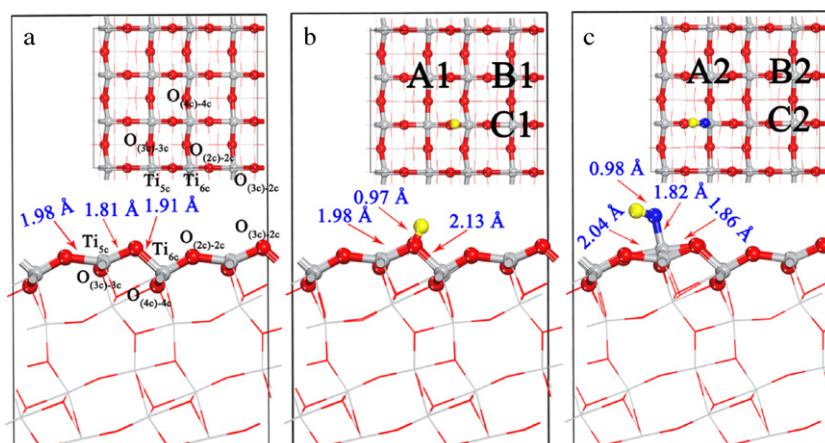


Fig. 1. Calculated structures of clean surface (a), hydroxylated surface with OH_{br} (b) and hydroxylated surface with OH_t (c). Only atoms exposed on the surface and atoms of adsorbate are shown in ball and stick model. Ti atoms and O atoms of TiO₂ are in gray and red, respectively. Atoms in the bulk with full coordination are shown in stick model. H atoms and O atoms of adsorbate are in yellow and blue, respectively. The non-equivalent Ti_{5c} sites around different hydroxyl groups are marked with A1–2, B1–2, C1–2 in each model. The bond lengths near hydroxyl group are also marked. (For interpretation of the references to color in this figure legend, the reader is referred to the web version of the article.)

tive surface with high surface energy. Vittadini et al. [24,25] also reported that TiO₂-B (100) is a very reactive surface and the dissociation of water is preferred on the surface. In this paper, we study the methanol adsorption behavior near the bridging and terminal hydroxyl groups to figure out how different hydroxyl groups impact on the chemisorption of methanol on TiO₂-B (100). Three kinds of bond scissions involving breaking O–H, C–O and C–H bonds are thoroughly studied at various non-equivalent sites around OH groups. Due to the obvious importance of the C–H scission of methanol, we give special focus to the C–H scission on the surface in this paper.

2. Computational details

Total energy calculations were performed within the framework of density functional theory (DFT). Kohn–Sham equation was solved by the self-consistent field method using PWscf code implemented in Quantum-Espresso 4.1.2 [26]. Since hydroxylated surfaces models contain an odd number of electrons, the spin-polarization effect is included in all the calculations. The generalized gradient approximation (GGA) with the Perdew–Wang 91 (PW91) functional was used to describe the exchange–correlation effects. The wave functions were expanded in terms of plane-wave basis set with cutoff energy of 30 Ry. Electron–ion interactions were described by ultrasoft pseudopotentials [27] with H 1s; C 2s, 2p; O 2s, 2p and Ti 3s, 3p, 3d, 4s electrons explicitly described as valence states.

The TiO₂-B (100) surface was modeled as periodic slabs of ~10.29 Å thickness plus 12 Å vacuum. Supercell of p(3 × 2) TiO₂-B (100) surface with dimensions of ~13.16 Å × 11.21 Å × 22.32 Å was used to avoid interactions of adsorbate molecules from mirror image. During all the calculations, the bottom half was fixed at the bulk position. Only atoms in the upper half of the slab and adsorbate were relaxed until the forces on free atoms were below 0.03 eV/Å. Because of the large dimensions of the supercell, k point sampling was restricted to the Γ point. The preliminary test calculations with 2 × 2 × 1 k-point sampling showed that denser Brillouin zone sampling could give very consistent results in energy and structure parameters. The adsorption energies of methanol on the surface were calculated using Eq. (1).

$$E_{\text{ads}} = E_{\text{methanol/surf}} - E_{\text{surf}} - E_{\text{methanol}} \quad (1)$$

where E_{ads} is the adsorption energy of methanol; $E_{\text{methanol/surf}}$, E_{surf} and E_{methanol} are the energies of the relaxed slab with methanol adsorbed on the surface (hydroxylated or clean), the hydroxylated or clean surface slab and isolated methanol molecule in the vacuum, respectively.

Considering that only one bond is broken in the initial dissociative adsorption of methanol, constrained minimization technique [28–30] was used to estimate the energy barrier of different kinds of bond scission at various sites. During the minimization, we constrained the length of the chemical bond to be broken at several values interpolated between the bond lengths before and after the dissociation. The upper half of the slab and adsorbate atoms are allowed to relax, so that the adsorbate molecules could be free to rotate and translate with only one bond constrained. The minimum energy paths (MEP) for dissociation as a function of bond length could be mapped out via plotting the total energies against the corresponding bond length constrained at different values. The energy barrier was calculated by comparing the total energy at the saddle point on the MEP curve and the molecular mode.

3. Results and discussion

3.1. Clean and hydroxylated TiO₂-B (100) surfaces

3.1.1. Clean TiO₂-B (100) surface

The clean (100) surface shows a very corrugated structure (~2.07 Å) and exposes two-/three-/four-coordinated O atoms (O_{(3c)-2c}, O_{(2c)-2c}, O_{(3c)-3c}, and O_{(4c)-4c}), together with five-/six-coordinated Ti atoms (Ti_{5c}/Ti_{6c}). The [O_{(3c)-2c}–Ti_{5c}–O_{(2c)-2c}–Ti_{6c}] chains arranged along [001] exhibit long stepped structure (~6.6 Å) (the part with/without bracket in subscript means coordination number before (in bulk)/after (on the surface) the formation of surface). The inward relaxation of O_{(3c)-2c}, Ti_{5c} and outward relaxation of Ti_{6c}, O_{(2c)-2c}, transform the stepped profile into a wave-like structure, Fig. 1a. Our result for the (100) surface structure is nicely consistent with the most recent reported calculated structures of TiO₂-B [25]. There are two kinds of 2-coordinated O atom on the surface, Fig. 1a. They are O_{(3c)-2c} and O_{(2c)-2c}, which are 3-fold and 2-fold, respectively, in the bulk before the formation of surface.

3.1.2. Hydroxylated (100) surface

As Vittadini et al. [24] and we [22] reported recently, the TiO₂-B (100) surface is very reactive and water could dissociate

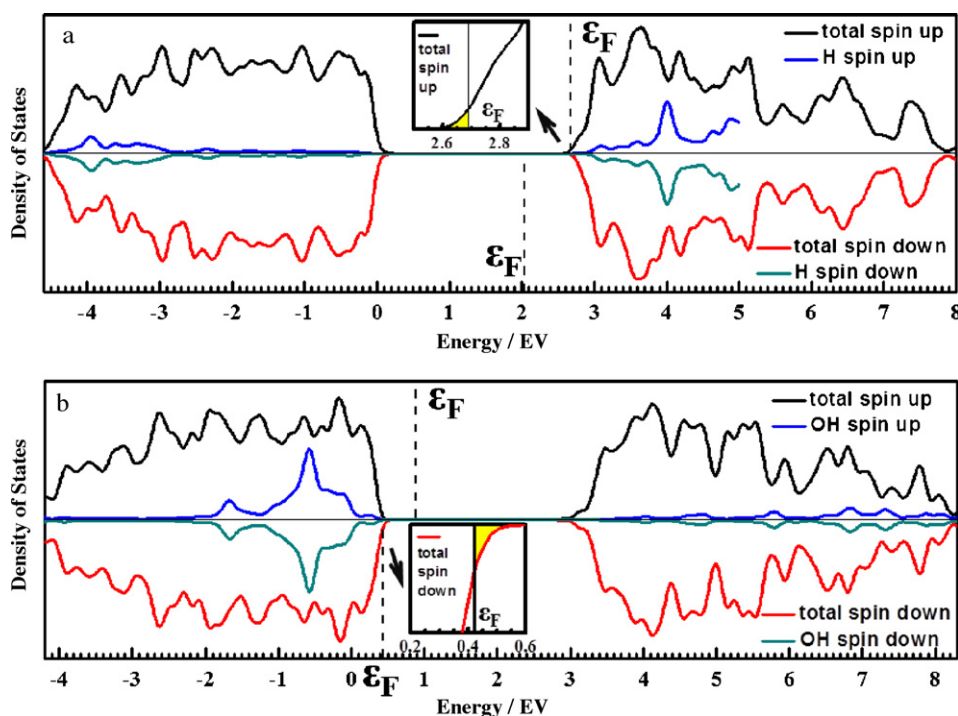


Fig. 2. Local density of states of surface exposed surface atoms for hydroxylated surface with (a) H_{br} and (b) H_t . The Fermi level is marked with vertical line at corresponding energy level. The LDOS of H and OH are amplified 250 and 5 times, respectively. Insets: magnified LDOS curves around the Fermi level.

spontaneously to form hydroxyl groups on the surface. After the dissociation of water, there are two kinds of hydroxyl groups on the surface, bridging hydroxyl group (OH_{br}), Fig. 1b, and terminal hydroxyl group (OH_t), Fig. 1c. The former is formed by H atom (H_{OH}) dissociated from water incorporating with bridging O anions of the solid surface (O_s); the latter is formed by OH fragment dissociated from water and coordinated to Ti_{5c} atom of the surface. Both hydroxyl groups could be detected by spectroscopic techniques on the TiO_2 surfaces [31,32]. The calculated O–H bond of OH_{br} and OH_t groups is 0.97 Å and 0.98 Å in this work. Because of the competition from the H adatom, the Ti–O bonds near OH_{br} are elongated to 1.98 Å and 2.13 Å from 1.81 Å and 1.91 Å. The OH_t binding to Ti_{5c} forms a Ti–O bond of 1.82 Å. Due to the adsorption of an OH_t , the Ti_{5c} bonded with OH_t is pulled out of the surface by ~ 0.5 Å.

By analysis of Lowdin charge and electron density difference, it could be inferred that the OH_{br} donates electrons to the TiO_2 surface. Introducing an OH_{br} can be called n-doping or reduction of the surface. Thus, the surface becomes an active reducing agent; In contrast, the OH_t extracts electrons from the surface. This can be considered as p-doping or oxidation of the surface. The TiO_2 surface with OH_t , thereby, has become an active oxidizing agent.

The local density of states (LDOS) of surface atoms for hydroxylated surface with OH_{br} and OH_t is recorded in Fig. 2a and b. The Fermi level, which is the boundary between the occupied level and the empty level, of spin up electrons is beyond the bottom of the conduction band on the hydroxylated surface with OH_{br} . This indicates the donated electrons by OH_{br} on the surface occupy the conduction band state, inset of Fig. 2a. The surface adsorbed H adatom contributes mainly to the conduction band and exhibits delocalized character. In contrast, on the hydroxylated surface with H_t the Fermi level shifted to lower energy. The Fermi level of spin down electrons shifted below the top of the valence band, inset of Fig. 2b, which suggests the extracted electrons identified by Lowdin charge and electron density difference analysis result in an empty electronic state. The adsorbed OH group contributes mainly to the valence band and also exhibits delocalized character.

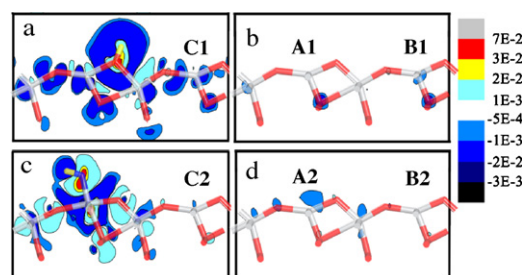


Fig. 3. Electron density difference contour plots indicating the redistribution of electron around bridging (a and b) and terminal OH (c and d) groups. Atoms near the surface are shown in the same color as Fig. 1. The non-equivalent Ti_{5c} sites around different hydroxyl groups are marked with the same labels. (For interpretation of the references to color in this figure legend, the reader is referred to the web version of the article.)

The contour map of electron density difference, Fig. 3, showed that the electronic structure around OH group is changed. The electron density (ED) on O atom of both of two kinds of OH is increased. The ED around H atoms of OH group is depleted. Both the OH_{br} and the OH_t result in the depletion of ED between Ti–O bonds near them, which causes the stretching of Ti–O bonds. The nearby Ti_{5c} sites also could be influenced by the OH groups, to some extent. The electronic structure of Ti_{5c} sites around hydroxyl groups, such as A1, B1, C1 and A2, B2, C2, are changed differently: The ED around O and Ti atoms at A2 and C1 sites is clearly reduced; The ED around Ti atoms at B1 and C2 sites is reduced a little; The ED around A1 and B2 is nearly unchanged.

The different electronic characters around various sites near the two kinds of OH groups might facilitate different kinds of reactions near them. To this end, we further study the methanol initial dissociation steps with OH_{br} and OH_t and compare them with the ones on the bare surface to identify the influence of different OH groups.

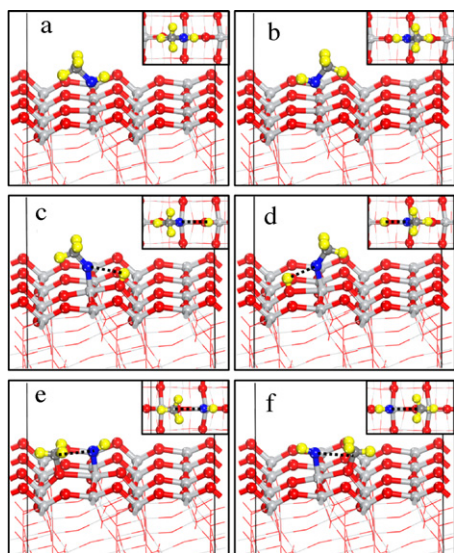
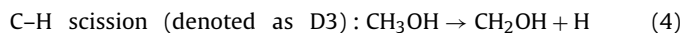
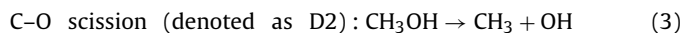
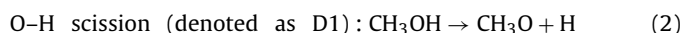


Fig. 4. Calculated structures of methanol adsorbed on bare $\text{TiO}_2\text{-B}$ (100) surface: Molecular adsorption (a, M.L.; b, M.R.); O–H activation (c, D1.L.; d, D1.R.); C–O activation (e, D2.L.; f, D2.R.). The broken bond in methanol is indicated by dashed line. The colors and models of atoms and bonds are the same as Fig. 1. (For interpretation of the references to color in this figure legend, the reader is referred to the web version of the article.)

3.2. Adsorption of methanol on clean $\text{TiO}_2\text{-B}$ (100)

Methanol adsorbed on clean $\text{TiO}_2\text{-B}$ (100) surface was calculated as a reference. Two stable configurations of methanol in the molecular state with CH_3 -group of methanol near $\text{O}_{(2c)-2c}$ and $\text{O}_{(3c)-2c}$, denoted as M.L and M.R, are identified at Ti_{5c} site on the surface. The configurations with CH_3 -group of methanol near $\text{O}_{(2c)-2c}$ and $\text{O}_{(3c)-2c}$ are denoted with postfix ‘L’ and ‘R’, respectively. (This notation is used all through this paper both for molecular and for dissociative states) The C–O bond in both of them arranges approximately along [001] direction. Adsorption energies are -0.94 eV and -0.96 eV for M.L and M.R shown in Fig. 4a and b, respectively. The distances between O of methanol and Ti_{5c} are 2.13 Å in both configurations. Because the adsorption energies of two adsorption structures are very similar, the probability of either could be equal when methanol adsorbed on the surface.

There are three kinds of activation of methanol at initial step described as,



The O–H and C–H scissions are important for applications aiming at directly using the hydrogen, such as production of H_2 or *in situ*

hydrogenation. The C–O scission is required for the synthesis of olefins, dimethyl ether, etc.

The above three initial activation steps are thoroughly considered on $\text{TiO}_2\text{-B}$ (100) surface. Based on the identified molecular adsorptions, M.L and M.R, two kinds of stable configurations for each activation process in dissociative states have been determined, Fig. 4c–f. In the O–H scission process, the H atom bonding to O in methanol (H_O) moves to the neighboring O_{2c} and the O atom of methanol (O_m) gets closer to Ti_{5c} on the surface to form Ti–O bond. The distances between O_m and Ti_{5c} in D1.L and D1.R are decreased to 1.79 Å and 1.82 Å, respectively, from 2.13 Å of molecularly adsorbed methanol on the surface (M.L and M.R), as shown in Table 1. The proton bonds to $\text{O}_{(2c)-2c}$ and $\text{O}_{(3c)-2c}$ with a distance of 0.97 Å and 0.98 Å in D1.L and D1.R, respectively. The adsorption energy of the most stable configuration (D1.L) with the proton binding to $\text{O}_{(3c)-2c}$ is -1.39 eV, which is about 0.31 eV more favorable than D1.R configuration with proton binding to $\text{O}_{(2c)-2c}$. The C–O activation process shows a similar behavior with O–H activation. During the C–O activation, the positive charged fragment, CH_3 group, moves to adjacent O_{2c} , both $\text{O}_{(2c)-2c}$ and $\text{O}_{(3c)-2c}$, on the surface and the OH group remains at the Ti_{5c} site. The D2.R configuration, Fig. 4f, with CH_3 binding to $\text{O}_{(3c)-2c}$ is more favorable than D2.L with CH_3 binds to $\text{O}_{(2c)-2c}$ (-1.24 eV vs. -0.49 eV). The D2.L with CH_3 bound to $\text{O}_{(2c)-2c}$ exhibits even lower stability than molecular adsorption. In both O–H and C–O scissions, the $\text{O}_{(3c)-2c}$ show superior activities than $\text{O}_{(2c)-2c}$ to accept dissociated fragments with positive charge of methanol.

Although the adsorptions of molecular states with different orientations, M.L and M.R, are nearly equal and the possibility of them is almost the same, they could lead to further O–H and C–O activation with different stabilities: The M.L configuration in the molecular state could lead to more favorable O–H activation; while the M.R configuration could lead to more feasible C–O activation from a thermodynamic viewpoint. This might be an indication of different selectivity caused by the orientation of molecular adsorption. It also should be mentioned that both most stable dissociative adsorptions via O–H and C–O activation are more stable than methanol molecularly adsorbed on the surface. This suggests the dissociation of methanol is very favorable on clean $\text{TiO}_2\text{-B}$ (100) surface.

The energy barriers for dissociation via O–H and C–O bond scission are further determined using constrained minimization technique. Although the adsorption energies differ very much in different orientations for both O–H and C–O dissociation, the activation barriers are nearly the same, Table 1. The activation energy for C–O scission is significantly larger than O–H scission, which indicates the O–H activation is much easier than C–O activation from a kinetic viewpoint.

The dissociation of methanol via C–H activation described in Eq. (4) is not stable on the surface. When the H atom of CH_3 group in methanol was separated manually and placed to first nearest O_{2c} sites along [001] in initial guess, the H atom came back to

Table 1

Calculated structural parameters and adsorption energies (E) of molecularly and dissociatively adsorbed methanol via different bond scissions on bare $\text{TiO}_2\text{-B}$ (100).

	E/eV	$r1^b/\text{Å}$	$r2^c/\text{Å}$	$r3^d/\text{Å}$	EB^a/eV	Label
Molecular adsorption	-0.94	2.13	–	–	–	M.L
	-0.96	2.13	–	–	–	M.R
Dissociation via O–H scission	-1.39	1.79	0.97	–	0.26	D1.L
	-1.08	1.82	0.98	–	0.21	D1.R
Dissociation via C–O scission	-0.49	1.83	–	1.46	1.17	D2.L
	-1.24	1.83	–	1.45	1.20	D2.R

^a EB denotes energy barrier.

^b $r1$ denotes the distance between the O atom of methanol and the Ti_{5c} atom on the surface.

^c $r2$ denotes the distance between the dissociated H atom of methanol and the O_{2c} atom on the surface.

^d $r3$ denotes the distance between the C atom of dissociated CH_3 group and the O_{2c} atom on the surface.

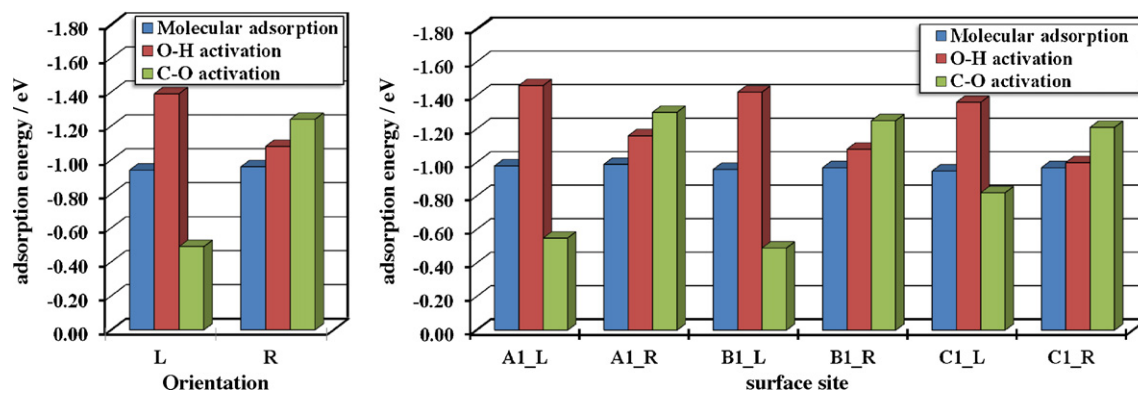


Fig. 5. Adsorption energies of methanol adsorbed in molecular state (blue bar) and dissociative state with C–O (red bar) and O–H (green bar) activation in different orientations at various sites near the bridging OH group. Left panel, on clean surface; right panel, on hydroxylated surface with OH_{br}. (For interpretation of the references to color in this figure legend, the reader is referred to the web version of the article.)

form molecular adsorption of methanol on the surface. If we further place the H atom of CH₃ group in methanol to second nearest O_{2c} sites along [001] in initial guess, the calculated adsorption energies for the two orientations both became positive, indicating an endothermic process. This is consistent with the results of methanol adsorbed on anatase (101) surface [10].

In general, by calculating the molecular and dissociative adsorption via O–H, C–O and C–H scissions on the clean surface, we could conclude that the methanol adsorption on clean TiO₂-B (100) is a chemisorption and the dissociation via O–H scission are more feasible than C–O and C–H scissions. This result is quantitatively consistent with results on other TiO₂ surfaces [17–19].

3.3. Adsorption of methanol on hydroxylated TiO₂-B (100)

Methanol adsorbed at different sites near two kinds of hydroxyl groups is studied to determine the effect of hydroxyl groups on the initial dissociation step of methanol on the surface.

3.3.1. Methanol dissociation near bridging OH groups

As marked in Fig. 1b, there are three nonequivalent sites near OH_{br} groups, denoted as A1, B1 and C1. We have thoroughly

checked the configurations of methanol both molecularly and dissociatively adsorbed at each site. Like on the clean surface, methanol could adsorb molecularly in two orientations, 'L' and 'R', at Ti_{5c} sites. The adsorption energies of methanol adsorbed in the molecular and dissociative state with C–O and O–H scission are summarized in Fig. 5 and Table 2. The prefix, A1, B1, C1, indicates the different sites marked in Fig. 1b. By comparing the adsorption energy and structural parameters on the clean with hydroxylated surface with OH_{br}, OH_{br} have little impact on the molecular adsorptions of methanol. The adsorption energies of methanol adsorbed in the molecular state near various sites are in range of –0.95 eV to –0.99 eV, which is approximately equal to the ones for the molecular adsorption at the bare surface (–0.94 eV for M.L and –0.96 eV for M.R). The structural parameter is very similar at different sites, as shown in Table 2. Selected configurations with higher adsorption energy are shown in Fig. 6 a and b.

The dissociative adsorptions are also not significantly affected by the OH_{br}. The adsorption energies of methanol in dissociative state via O–H with 'L' and 'R' orientation are in range of –1.36 eV to –1.46 eV and –1.00 eV to –1.16 eV. The O–H activation is easier at A1 and B1 sites with a bit lower energy barrier, Table 2. At C1 site, the O–H activation is affected by the OH_{br} a little and the activation barrier becomes larger than 0.30 eV.

Table 2
Calculated structural parameters and adsorption energies (*E*) of molecularly and dissociatively adsorbed methanol via different bond scissions on TiO₂-B (100) surface with OH_{br}.

	<i>E</i> /eV	<i>r</i> ^a /Å	<i>r</i> ^b /Å	<i>r</i> ^c /Å	<i>r</i> ^d /Å	EB ^e /eV	Label
Molecular adsorption	–0.98	2.13	–	–	0.97	–	A1.M.L
	–0.99	2.13	–	–	0.97	–	A1.M.R
	–0.96	2.12	–	–	0.97	–	B1.M.L
	–0.97	2.12	–	–	0.97	–	B1.M.R
	–0.95	2.13	–	–	0.98	–	C1.M.L
	–0.97	2.12	–	–	0.98	–	C1.M.R
Dissociation via O–H scission	–1.46	1.79	0.97	–	0.98	0.21	A1.D1.L
	–1.16	1.82	0.98	–	0.98	0.15	A1.D1.R
	–1.42	1.79	0.97	–	0.98	0.22	B1.D1.L
	–1.08	1.82	0.98	–	0.98	0.14	B1.D1.R
	–1.36	1.79	0.97	–	0.98	0.33	C1.D1.L
	–1.00	1.81	0.98	–	0.98	0.39	C1.D1.R
Dissociation via C–O scission	–0.55	1.84	–	1.46	0.97	1.04	A1.D2.L
	–1.30	1.83	–	1.45	0.98	1.16	A1.D2.R
	–0.49	1.83	–	1.46	0.98	1.07	B1.D2.L
	–1.25	1.83	–	1.45	0.98	1.14	B1.D2.R
	–0.82	1.83	–	1.43	0.97	1.13	C1.D2.L
	–1.21	1.83	–	1.44	0.98	1.11	C1.D2.R

^a *r*₁ denotes the distance between the O atom of methanol and the Ti_{5c} atom on the surface.

^b *r*₂ denotes the distance between the dissociated H atom of methanol and the O_{2c} atom on the surface.

^c *r*₃ denotes the distance between the C atom of dissociated CH₃ group and the O_{2c} atom on the surface.

^d *r*₄ denotes the distance between the H atom of bridging OH group and the O_{2c} atom on the surface.

^e EB denotes energy barrier.

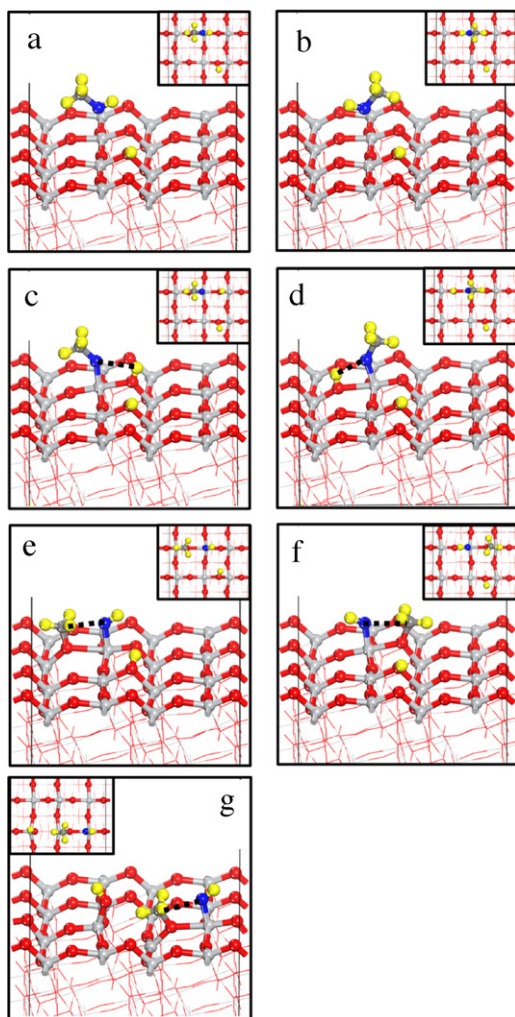


Fig. 6. Selected calculated stable structures of methanol adsorbed on hydroxylated $\text{TiO}_2\text{-B}$ (100) surface with OH_{br} : molecular adsorption (a, A1.M.L; b, A1.M.R); O–H activation (c, A1.D1.L; d, A1.D1.R); C–O activation (e, A1.D2.L; f, A1.D2.R; g, C1.D2.L). The broken bond in methanol is indicated by dashed line. The colors and models of atoms and bonds are the same as Fig. 1. (For interpretation of the references to color in this figure legend, the reader is referred to the web version of the article.)

Meanwhile, adsorption energies are in range of -0.49 eV to -0.82 eV and -1.21 eV to -1.30 eV for the C–O scission process with 'L' and 'R' orientation, respectively. Since most of the configurations of dissociative states via O–H or C–O scission exhibit nearly similar adsorption style of methanol at different sites, Table 2, only selected calculated configurations with higher adsorption energies are shown in Fig. 6c–f. These results are nearly the same as the results on the clean $\text{TiO}_2\text{-B}$ (100) surface. The relative stability at various sites with different orientations on the hydroxylated surface with OH_{br} is the same as that on the clean surface, except for C1.D2.L configuration, Fig. 6g. At C1 site with 'L' orientation, the C–O scission process is enhanced by 0.33 eV. Because the positive charged dissociated fragment, CH_3 group, of methanol is too close to the H_{OH} atom of OH_{br} , one of Ti–O bonds is broken and OH_{br} moves away from the dissociated CH_3 group to minimize the repulsion between two H atoms. The C–O scissions with the 'R' orientation, and on other sites are showing nearly the same behavior as on the clean surface with no obvious bond breaking on the solid surface, Fig. 6a–f. Thus, the special enhancement of C–O scission in 'L' orientation at C1 site could be considered as structural induced profile. The C–O activation barriers at different sites near the OH_{br}

are around 1.10 eV, a little lower than those on the clean surface. As on the clean surface, the C–O activation is still much harder to occur due to the kinetic limit.

The C–H scission on the surface with OH_{br} is identical to the result of clean surface. If the dissociated H_{m} moves to first nearest $\text{O}_{2\text{c}}$ along [001], the C–H bond recovered very easily and formed molecular adsorption again. Even when the H_{m} atom of CH_3 group of methanol moves to second nearest $\text{O}_{2\text{c}}$ along [001], the calculated configuration is very unstable with positive adsorption energy. Thus, the C–H scission is still not feasible on the hydroxylated surface with OH_{br} .

3.3.2. Methanol dissociation near terminal OH groups

There are three nonequivalent sites near the OH_{t} as well, denoted as A2, B2 and C2 in Fig. 1c. The molecular and dissociative adsorptions with different orientations and bond scissions are calculated at these sites. The adsorption energies of methanol adsorbed in the molecular and dissociative state with C–O, O–H and C–H scissions are summarized in Fig. 7 and Table 3. The prefix A2, B2, C2, indicates the different sites marked in Fig. 1c. The adsorption energies of the methanol adsorbed in the molecular state are in range of -0.89 eV to -0.95 eV, which is almost the same as that on the clean and hydroxylated surface with OH_{br} . The adsorption energies in ranges of -1.34 eV to -1.38 eV and -1.02 eV to -1.16 eV for dissociative adsorptions via O–H scission with 'L' and 'R' orientations and those in range of -0.39 eV to -0.60 eV and -1.18 eV to -1.23 eV for dissociative adsorptions via C–O scission with 'L' and 'R' orientations are also nearly the same as the case on clean surface. Unlike the dissociative adsorption via C–O scission at C1 site with 'L' orientation, the C–O scission at C2 site with 'L' orientation shows no obvious enhancement with respect to the one on the clean surface. Consequently, just as on the hydroxylated surface with OH_{br} group, the molecular and dissociative adsorptions via O–H and C–O scissions are also not significantly affected by the OH_{t} groups. The activation barriers for O–H and C–O dissociation are around ~ 0.25 eV and ~ 1.20 eV, respectively, nearly identical to the results on the clean and hydroxylated surface with H_{br} , Table 3.

Very interestingly, we found the C–H scission is greatly strengthened near the OH_{t} on the surface. Two mechanisms have been identified: One is the H atom of CH_3 group (H_{C}) in methanol is dissociated to nearest $\text{O}_{2\text{c}}$ sites along [001] (denoted as 'F' mechanism); the other is the H_{C} dissociating to next nearest $\text{O}_{2\text{c}}$ sites along [001] and the C atom bonded to nearest $\text{O}_{2\text{c}}$ sites along [001] (denoted as 'S' mechanism).

Unlike the situation on the clean surface and the hydroxylated surface with OH_{br} group, the H_{C} in methanol dissociates to the nearest $\text{O}_{2\text{c}}$, both $\text{O}_{(2\text{c})-2\text{c}}$ and $\text{O}_{(3\text{c})-2\text{c}}$, with negative adsorption energies in range of -0.67 eV to -1.00 eV. Since the structural parameters are very similar at different sites, as shown in Table 3, only selected configurations with higher adsorption energies are shown in Fig. 8a and b. During the C–H scission process, the CH_2 group of CH_2OH rotates to make the atoms of CH_2OH almost in the same plane and perpendicular to the surface and the H_{C} moves to nearest $\text{O}_{2\text{c}}$ and rotates into the surface. Because of the obviously exothermic characteristic of dissociation via C–H session in the 'F' mechanism, the dissociated H_{C} could bind to the $\text{O}_{2\text{c}}$ rather than recombine with the CH_2OH fragment and form molecularly adsorbed methanol. The activation barrier referring to the molecular mode for C–H dissociation is in range of 0.60 – 0.81 eV, the absolute value of which is slightly lower than the adsorption energy of molecular adsorption. This indicates the dissociation of C–H could be finished before the molecule desorbed from the surface.

During the C–H scission process following the 'S' mechanism, the H_{C} of methanol moves to the second nearest $\text{O}_{2\text{c}}$ along [001] and the negative fragments, CH_2OH , get closer to the surface with C atom binding to the first nearest $\text{O}_{2\text{c}}$ atoms. Selected calculated

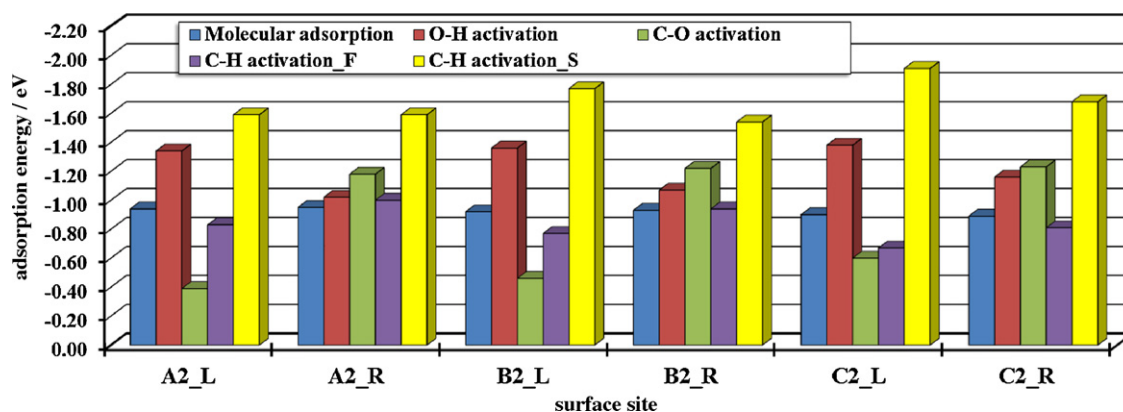


Fig. 7. Adsorption energies of methanol adsorbed in molecular state (blue bar) and dissociative state with O–H (red bar), C–O (green bar), C–H (purple for mechanism F; yellow for mechanism S) cleavages in different orientations at various sites near the OH_t group. (For interpretation of the references to color in this figure legend, the reader is referred to the web version of the article.)

configurations with higher adsorption energies of each orientation are shown in Fig. 8c–e. The H_C is accepted by more reactive site, O_{(3c)-2c}, in the dissociative adsorption via C–H scission with ‘L’ orientation, Fig. 8c. Accepting the H_C, the O_{(3c)-2c} is broken away from the Ti_{5c} cation upon the chemi-sorption of methanol at A2 and B2 sites. The adsorption energies for these two configurations are 1.59 eV and 1.77 eV. While, at C2 site, the adsorption energy for methanol dissociatively adsorbed with ‘L’ orientation is 1.91 eV. At C2 site, Fig. 8e, the O_{(3c)-2c} is still bonded with Ti_{5c} upon acceptance of H_C because of the effect of OH_t along [001]. In dissociative adsorption with ‘R’ orientation, the H_C coordinates to O_{(2c)-2c} with no obvious bond breaking of solid surface. The adsorption ener-

gies for methanol dissociatively adsorbed via C–H scission with ‘R’ orientation at different sites are in range of –1.59 to –1.68 eV. It should be noticed that the C–H scission of methanol around the OH_t could result in extraordinarily low adsorption energy and stable structure of chemi-sorption of methanol. In other words, the hydroxylated surface with H_t could be stabilized by the C–H dissociation of methanol. Thus, the C–H scission following ‘S’ mechanism is enhanced significantly around the OH_t. Although the intermediate product of C–H bond scission following S mechanism is more stable than the one following F mechanism, the energy barrier for this dissociation is larger. The activation energy barriers for C–H activation are different from site to site, ranging from 0.80 eV to 1.34 eV,

Table 3
Calculated structural parameters and adsorption energies (*E*) of molecularly and dissociatively adsorbed methanol via different bond scissions on TiO₂-B (1 0 0) surface with OH_t.

	<i>E</i> /eV	r1 ^a /Å	r2 ^b /Å	r3 ^c /Å	r5 ^d /Å	EB ^e /eV	Label
Molecular adsorption	–0.94	2.12	–	–	1.83	–	A2.M.L
	–0.95	2.12	–	–	1.83	–	A2.M.R
	–0.92	2.12	–	–	1.82	–	B2.M.L
	–0.93	2.12	–	–	1.82	–	B2.M.R
	–0.90	2.12	–	–	1.82	–	C2.M.L
	–0.89	2.13	–	–	1.83	–	C2.M.R
Dissociation via O–H scission	–1.34	1.79	0.97	–	1.82	0.29	A2.D1.L
	–1.02	1.81	0.98	–	1.82	0.21	A2.D1.R
	–1.36	1.79	0.97	–	1.82	0.28	B2.D1.L
	–1.07	1.82	0.98	–	1.82	0.22	B2.D1.R
	–1.38	1.80	0.97	–	1.82	0.21	C2.D1.L
	–1.16	1.82	0.98	–	1.82	0.22	C2.D1.R
Dissociation via C–O scission	–0.39	1.83	–	1.46	1.82	1.15	A2.D2.L
	–1.18	1.83	–	1.44	1.82	1.09	A2.D2.R
	–0.46	1.83	–	1.46	1.82	1.11	B2.D2.L
	–1.22	1.83	–	1.44	1.82	1.22	B2.D2.R
	–0.60	1.84	–	1.45	1.82	1.00	C2.D2.L
	–1.23	1.83	–	1.43	1.82	1.23	C2.D2.R
Dissociation via C–H scission, F mechanism	–0.83	2.20	0.99	–	1.83	0.63	A2.D3.L
	–1.00	2.22	0.98	–	1.84	0.60	A2.D3.R
	–0.77	2.20	0.99	–	1.82	0.70	B2.D3.L
	–0.94	2.19	0.98	–	1.82	0.81	B2.D3.R
	–0.67	2.20	0.99	–	1.82	0.71	C2.D3.L
	–0.81	2.19	0.98	–	1.82	0.79	C2.D3.R
Dissociation via C–H scission, S mechanism	–1.59	2.16	0.98	1.38	1.82	0.99	A2.D4.L
	–1.59	2.16	0.99	1.37	1.82	1.25	A2.D4.R
	–1.77	2.16	0.98	1.37	1.83	1.15	B2.D4.L
	–1.54	2.16	0.99	1.37	1.82	1.33	B2.D4.R
	–1.91	2.17	0.98	1.39	1.83	1.33	C2.D4.L
	–1.68	2.16	0.99	1.37	1.83	0.80	C2.D4.R

^a r1 denotes the distance between the O atom of methanol and the Ti_{5c} atom on the surface.

^b r2 denotes the distance between the dissociated H atom of methanol and the O_{2c} atom on the surface.

^c r3 denotes the distance between the C atom of dissociated CH₃ group and the O_{2c} atom on the surface.

^d r5 denotes the distance between the O atom of terminal OH group and the Ti_{5c} atom on the surface.

^e EB denotes energy barrier.

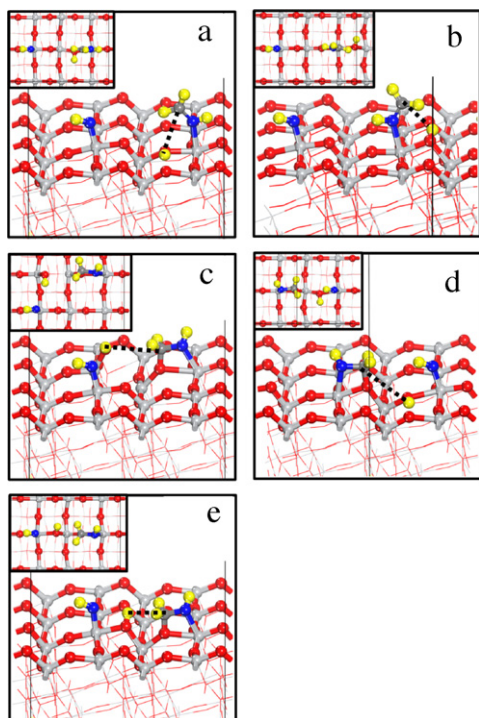


Fig. 8. Selected calculated stable structures of methanol dissociatively adsorbed via C–H bond scissions near OH_t group on hydroxylated $\text{TiO}_2\text{-B}$ (100) surface: (a) 'L' orientation at C2 site and (b) 'R' orientation at C2 site following 'F' mechanism; (c) 'L' orientation at B2 site and (d) 'R' orientation at C2 site following 'S' mechanism; (e) 'L' orientation at C2 site following 'S' mechanism. The colors and models of atoms and bonds are same as Fig. 1. (For interpretation of the references to color in this figure legend, the reader is referred to the web version of the article.)

Table 3. The lowest energy barrier for C–H activation, 0.80 eV, could be achieved at C2 site in 'R' orientation.

In contrast to the O–H and C–O scissions, the C–H scission will lead to oxidation of the C atom in methanol. As it was remarked before that since the OH_t group could extract electrons from the surface and result in an empty electronic state close to the valence band edge, the surface with OH_t has an oxidizing feature. Thereby, the extraordinarily low adsorption energy and stable structure of chemisorption of methanol via C–H scission would originate from the oxidizing character of the surface site around the OH_t on the surface.

However, only a few investigations implied direct evidence of the existence of OH_t on TiO_2 surface [33–36]. According to most of the previous investigations on surface chemistry of TiO_2 , the p-doped surfaces are hard to be stabilized under normal circumstances because of the well-known difficulty in making p-doped oxides. The electron-deficient p-doped state might be quenched by other defects which act as the electron donor, such as the O vacancies, Ti interstitials, or Hydrogen impurities. Therefore, the OH_t on the surface could be short lived. Our results demonstrate that if the local structures of $\text{TiO}_2\text{-B}$ (100) surface with OH_t could be efficiently stabilized, this will be very promising for interesting properties, such as the calculations of the present study show.

3.4. Transport of proton in methanol to the surface via terminal OH group

Having Brønsted acid character, the terminal OH group has been presumed as the proton channel on the surface [4]. It could be confirmed in Fig. 3c that the O atom in OH_t could be the hot spot to accept H atoms dissociated from methanol because of the obvious electron surplus feature around it. To understand the molecular

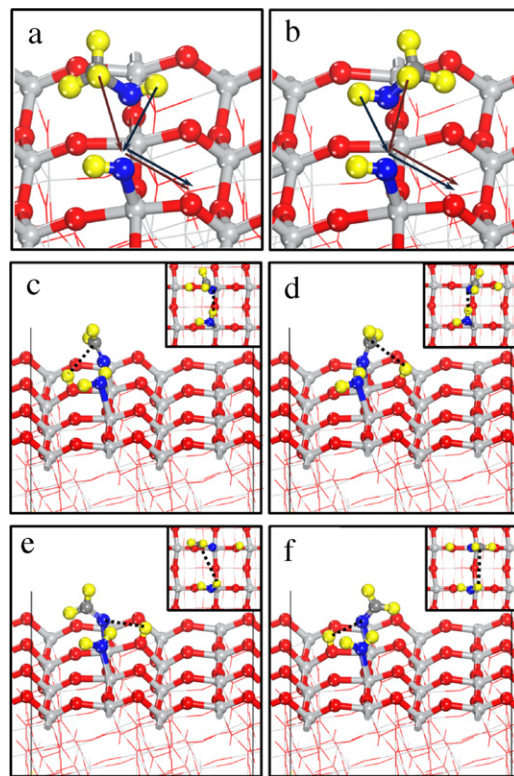


Fig. 9. Scheme of proton migration from methanol to surface: a and b for L and R orientation; stable structures of the migration of proton to OH_t : c and d for H_0 to OH_t in L and R orientation; e and f for H_C to OH_t in L and R orientation.

detail of the proton channel feature of the basic OH_t on the surface, we perform further calculations on the proton transfer behavior from methanol to OH_t .

Since the A2 site is very close to OH_t , it is the most probable hot spot for the proton transfer process, Fig. 9a and b. When the H atom bonding to O atom (H_0) in methanol adsorbed at A2 site is transferred to OH_t , further C–H scission of the remaining fragment, CH_3O , readily occurs and formaldehyde (CH_2O) is produced on the surface, Fig. 9c and d. The adsorption energies for L and R orientation are -1.39 eV and -1.81 eV, respectively. When the H atom bonding to C (H_C) in methanol is transferred to OH_t , Fig. 9e and f, further O–H bond breaking and production of formaldehyde is even more favorable with adsorption energies of -1.81 eV and -1.51 eV for L and R orientation, respectively. This again confirms that the $\text{O}_{(3c)-2c}$ anion is more reactive than $\text{O}_{(2c)-2c}$ to accept positive fragment dissociated from methanol. By comparing the stability of different configurations, it could be concluded that the H_C could be more preferable to migrate to OH_t at initial step. More importantly, after H atom transferred to the OH_t , the remaining fragment, CH_3O , would be so reactive that formaldehyde which was supposed to generate under UV radiation [4] could be produced with the help of OH_t on $\text{TiO}_2\text{-B}$ (100). To some extent, the holes generated by introducing an OH_t are nearly equal to the holes excited by UV radiation.

After the H atom, either H_C or H_0 , is accepted by OH_t , the water molecule is formed. The regeneration of OH_t via the further dissociation of water is calculated to identify the ability of recovery of the hydroxyl group and the migration of proton. By separating the H atom accepted by OH_t and putting it on the surface O_{2c} site, we find the adsorption energies are further decreased: Adsorption energies for the H_0 atom further migrates from OH_t to surface $\text{O}_{(3c)-2c}$, shown in Fig. 10a and b, are -1.78 eV and -2.23 eV for L and R orientation. Further migration of H_C to surface, shown in Fig. 10c and d, is even

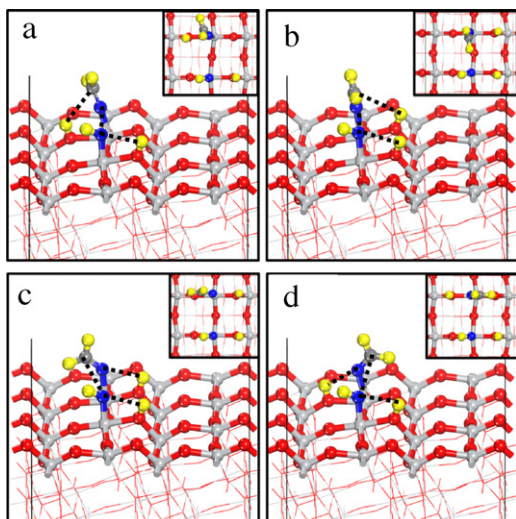


Fig. 10. Regeneration of OH_t and further migration of proton from OH_t to surface: a and b for H_O to surface; c and d for H_C to surface.

more favorable and lead to larger stability. The adsorption energies of them are -2.23 eV and -1.93 eV for L and R orientation. This indicates the migration of proton to the surface from OH_t could result in larger stability of the system. As we reported previously, the water molecule is very reactive on $\text{TiO}_2\text{-B}$ (100). Thus, the reactivity of $\text{TiO}_2\text{-B}$ (100) surface should be the leading cause of this superior ability of recovery of the hydroxyl group and the migration of proton.

4. Conclusions

In this work, we have performed first principle calculations to study the methanol adsorption via various bond scissions in different orientations on both clean and hydroxylated $\text{TiO}_2\text{-B}$ (100) surface with OH_{br} or OH_t groups. Spontaneous dissociation of methanol is identified as the main character on both clean and hydroxylated $\text{TiO}_2\text{-B}$ (100) surface. The O–H scission is found to be the most favorable dissociation style on the both on the clean and on the hydroxylated surface with bridging OH group. Thus, the OH_{br} has little influence on the adsorption of methanol. Interestingly, the terminal hydroxyl group has a great effect on the C–H scission, which is previous believed to be not feasible at all on the clean TiO_2 surfaces. The C–H scission is identified as the most preferential dissociation with extremely low adsorption energy on the surface with OH_t . Meanwhile, the hydrogen atoms in methanol are easy to transfer on the surface with the help of OH_t . Therefore, the terminal hydroxyl group could be regarded as the proton channel on the surface.

Acknowledgements

We are very grateful to anonymous reviewers whose careful examination of our manuscript, constructive suggestions and rigorous comments resulted in a considerable improvement of

this paper. We also gratefully acknowledge the guest editor, Prof. Qingfeng Ge (Southern Illinois University, IL), for his careful examination of our manuscript and all the help given to us.

This work was supported by NSFC-RGC Joint Research Award (No. 20731160614) and Changjiang Scholars and Innovative Research Team in University (No. PCSIRT0732). The authors also acknowledge the financial support from National Natural Science Foundation of China (Nos. 20736002, 20706029, 20876073, and 20906081) and National Basic Research Program of China (No. 2009CB226103, 2009CB623400 and 2009CB219902).

References

- [1] G.A. Olah, Angew. Chem. Int. Ed. 44 (2005) 2636–2639.
- [2] G.A. Olah, A. Goepfert, G.K. Surya Prakash, Beyond Oil and Gas: The Methanol Economy, 2nd ed., WILEY-VCH Verlag GmbH & Co. KGaA, Weinheim, 2009.
- [3] Y. Xiang, Q. Meng, X. Li, J. Wang, Chem. Commun. 46 (2010) 5918–5920.
- [4] J.G. Highfield, M.H. Chen, P.T. Nguyen, Z. Chen, Energy Environ. Sci. 2 (2009) 991–1002.
- [5] C.-M. Wang, Y.-D. Wang, Z.-K. Xie, Z.-P. Liu, J. Phys. Chem. C 113 (2009) 4584–4591.
- [6] M.P. Atkins, M.J. Earle, K.R. Seddon, M. Swadźba-Kwaśny, L. Vanoye, Chem. Commun. 46 (2010) 1745–1747.
- [7] Y. Fu, J. Shen, Chem. Commun. (2007) 2172–2174.
- [8] J. Kiss, A. Witt, B. Meyer, D. Marx, J. Chem. Phys. 130 (2009) 184706.
- [9] C.-M. Wang, K.-N. Fan, Z.-P. Liu, J. Am. Chem. Soc. 129 (2007) 2642–2647.
- [10] Y. Han, C.-j. Liu, Q. Ge, J. Phys. Chem. C 113 (2009) 20674–20682.
- [11] F.C. Meunier, ACS Nano 2 (2008) 2441–2444.
- [12] J.G. Yu, L.F. Qi, M. Jaroniec, J. Phys. Chem. C 114 (2010) 13118–13125.
- [13] W.-C. Lin, W.-D. Yang, I.L. Huang, T.-S. Wu, Z.-J. Chung, Energy Fuels 23 (2009) 2192–2196.
- [14] M.A. Henderson, Surf. Sci. Rep. 46 (2002) 1–308.
- [15] Y.-x. Pan, C.-j. Liu, Q. Ge, J. Catal. 272 (2010) 227–234.
- [16] Y. Pan, C.-j. Liu, Q. Ge, Langmuir 24 (2008) 12410–12419.
- [17] S.P. Bates, M.J. Gillan, G. Kresse, J. Phys. Chem. B 102 (1998) 2017–2026.
- [18] A. Tilotta, A. Selloni, J. Phys. Chem. B 108 (2004) 19314–19319.
- [19] X.Q. Gong, A. Selloni, J. Phys. Chem. B 109 (2005) 19560–19562.
- [20] R.H. Crabtree, Chem. Rev. 110 (2010) 575–1575.
- [21] S.S. Chen, Y.H. Zhu, W. Li, W.J. Liu, L.C. Li, Z.H. Yang, C. Liu, W.J. Yao, X.H. Lu, X. Feng, Chin. J. Catal. 31 (2010) 605–614.
- [22] W. Liu, J.-g. Wang, W. Li, X. Guo, L. Lu, X. Lu, X. Feng, C. Liu, Z. Yang, Phys. Chem. Chem. Phys. 12 (2010) 8721–8727.
- [23] W. Li, C. Liu, Y. Zhou, Y. Bai, X. Feng, Z. Yang, L. Lu, X. Lu, K.-Y. Chan, J. Phys. Chem. C 112 (2008) 20539–20545.
- [24] A. Vittadini, M. Casarin, A. Selloni, J. Mater. Chem. 20 (2010) 5871–5877.
- [25] A. Vittadini, M. Casarin, A. Selloni, J. Phys. Chem. C 113 (2009) 18973–18977.
- [26] P. Giannozzi, S. Baroni, N. Bonini, M. Calandra, R. Car, C. Cavazzoni, D. Ceresoli, G.L. Chiarotti, M. Cococcioni, I. Dabo, A. Dal Corso, S. Fabris, G. Fratesi, S. de Gironcoli, R. Gebauer, U. Gerstmann, C. Gougousis, M.L.A. Kokalj, L. Martin-Samos, N. Marzari, F. Mauri, R. Mazzarello, S. Paolini, A. Pasquarello, L. Paulatto, C. Sbraccia, S. Scandolo, G. Sclauzero, A.P. Seitsonen, A. Smogunov, P. Umari, R.M. Wentzcovitch, J. Phys.: Condens. Matter. 21 (2009) 395502.
- [27] We used the pseudopotentials, Ti.pw91-sp-van.ak.UPF, O.pw91-van.ak.UPF, C.pw91-van.ak.UPF and H.pw91-van.ak.UPF, from <http://www.quantum-espresso.org>.
- [28] A. Alavi, P. Hu, T. Deutsch, P.L. Silvestrelli, J. Hutter, Phys. Rev. Lett. 80 (1998) 3650–3653.
- [29] B. Hammer, K.W. Jacobsen, J.K. Nørskov, Phys. Rev. Lett. 69 (1992) 1971–1974.
- [30] L.M. Liu, B. McAllister, H.Q. Ye, P. Hu, J. Am. Chem. Soc. 128 (2006) 4017–4022.
- [31] K.S. Finnie, D.J. Cassidy, J.R. Bartlett, J.L. Woolfrey, Langmuir 17 (2001) 816–820.
- [32] D. Yang, H. Liu, Z. Zheng, Y. Yuan, J.-c. Zhao, E.R. Waclawik, X. Ke, H. Zhu, J. Am. Chem. Soc. 131 (2009) 17885–17893.
- [33] Y. Du, N.A. Deskins, Z. Zhang, Z. Dohnálek, M. Dupuis, I. Lyubnitsky, J. Phys. Chem. C 114 (2010) 17080–17084.
- [34] Y. Du, N.A. Deskins, Z. Zhang, Z. Dohnálek, M. Dupuis, I. Lyubnitsky, J. Phys. Chem. C 113 (2008) 666–671.
- [35] Z. Zhang, Y. Du, N.G. Petrik, G.A. Kimmel, I. Lyubnitsky, Z. Dohnálek, J. Phys. Chem. C 113 (2009) 1908–1916.
- [36] Y. Du, N.A. Deskins, Z. Zhang, Z. Dohnálek, M. Dupuis, I. Lyubnitsky, Phys. Rev. Lett. 102 (2009) 096102.